Composites Part B 223 (2021) 109115

Contents lists available at ScienceDirect

Composites Part B

journal homepage: www.elsevier.com/locate/compositesb

Synergistic effect of piperazine pyrophosphate and epoxy-octavinyl silsesquioxane on flame retardancy and mechanical properties of epoxy resin

Shansu Li [a], Yuan Liu [a,*], Yuansen Liu [b,**], Qi Wang [a]

[a] Polymer Research Institute of Sichuan University, The State Key Laboratory of Polymer Materials Engineering, Chengdu, 610065, China
[b] Technology Innovation Center for Exploitation of Marine Biological Resources, Third Institute of Oceanography, Ministry of Natural Resources, Xiamen, 361005, China

ARTICLE INFO

Keywords:
Epoxy resin
Synergistic effect
Flame retardancy
Mechanical properties
Smoke suppression

ABSTRACT

In order to solve the contradiction between the flame retardancy and mechanical properties of epoxy resin, piperazine pyrophosphate (PAPP) and epoxy-octavinyl silsesquioxane (EOVS) are applied as flame retardants for epoxy resin (EP). With the introduction of PAPP and EOVS, the properties of the EP composites about flame retardancy, mechanical properties and smoke suppression are significantly improved. EP/9 wt% PAPP/1 wt% EOVS (EP3) passes a vertical burning (UL-94) test V-0 rating and acquires the limiting oxygen index (LOI) test value of 32.4%. The results of cone calorimeter (CC) tests confirm that the incorporation of PAPP and EOVS significantly reduces the total heat release (THR), peak heat release (PHRR), total smoke production (TSP) and peak smoke produce rate (PSPR) values, which are respectively decreased by 25%, 81%, 57% and 63% compared with those of pure EP. Scanning electron microscope (SEM), energy dispersive spectrometry (EDS), Laser Raman spectroscopy (LRS), X-ray photoelectron spectroscopy (XPS) and Thermogravimetry-Fourier transform infrared (TG-FTIR) spectroscopy are adopted to analyze the flame-retardant mechanism of PAPP/EOVS flame retardants. These results reveal that the flame retardancy of EP3 is attributed to the excellent charring ability, the dilution effect of non-combustible gases and the flame inhibition of gaseous phosphorous compounds. Besides, the tensile and impact strength of EP3 increase benefitting from the presence of epoxy groups and Si-O bonds in EOVS. This work proposes a new method to prepare the mechanically reinforced and flame-retardant epoxy resin.

1. Introduction

As one of the most common thermosetting polymer plastics, epoxy resin is widely used in architectural coatings, integrated circuits, composites and aerospace fields owing to excellent adhesion, high mechanical strength, good corrosion resistance and low dielectric constant [1–4]. However, the high flammability of epoxy resin limits its practical application. When epoxy resin burns, it releases a large amount of black toxic smoke with the phenomenon of melting and dripping, which is easy to cause secondary combustion [5–8]. Therefore, it is necessary to modify the epoxy resin to be flame-retardant without sacrificing mechanical properties.

Due to the environmental-friendly requirements, halogen-free flame retardants including phosphorous-, nitrogen-, and silicon-based flame retardants [9–15] have attracted more attention. Actually, the single flame retardant usually restricts the further improvement of flame retardancy for epoxy resin. Some researches [16–18] have shown that the flame retardancy of epoxy resin can be further enhanced by introducing flame-retardant compositions containing multiple functional groups, such as maleimide, triazintrione, phenanthrene, phosphazene, silsesquioxane, etc. Therefore, combining different functional groups with certain flame retardants through physical blending or chemical reaction is a feasible method to efficiently improve the flame retardancy of epoxy resin.

Piperazine pyrophosphate (PAPP) is a halogen-free additive flame retardant that has attracted high attention in recent years. PAPP can be used in polypropylene, polyamide, epoxy resin and elastomer due to the preparation green, high thermal decomposition temperature and excellent carbonization performance [19–24]. PAPP is a single-component intumescent flame retardant containing phosphorus

* Corresponding author.
** Corresponding author.
E-mail address: liuyuan42001@163.com (Y. Liu).

https://doi.org/10.1016/j.compositesb.2021.109115
Received 20 April 2021; Received in revised form 14 June 2021; Accepted 29 June 2021
Available online 30 June 2021

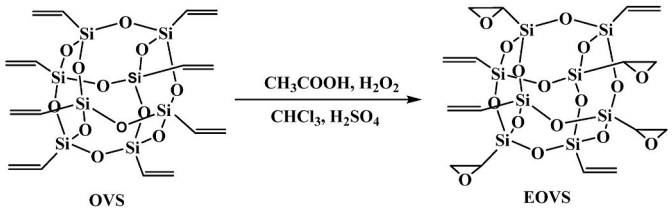

Scheme 1. The synthetic route of EOVS.

and nitrogen, which can inhibit the continuous burning of materials in the gas phase and condensed phase. Sun et al. [22] reported that the UL-94 test of 20 wt% PAPP/EP composite reached the V-0 level, but the higher content of additive flame retardant affected the mechanical properties of epoxy resin. Therefore, it's necessary to explore more efficient synergistic flame-retardant systems for enhancing the flame retardancy and mechanical properties of epoxy resin.

Polyhedral oligomeric silsesquioxane (POSS) is a kind of popular inorganic-organic hybrid material. The cage core of POSS is mainly composed of -Si-O-Si- bonds and the existence of inorganic chemical bonds makes it have good heat resistance and mechanical properties [25,26]. The eight external organic functional groups of POSS can be designed as epoxy groups, amine groups, hydroxyl groups [27–34], etc. POSS bonds with other organic polymers through organic functional groups, and form a cross-linked network structure with good compatibility. Based on the previous research, it is feasible to oxidize the vinyl groups to epoxy groups on octavinyl silsesquioxane (OVS), but eight reactive groups on OVS may be incompletely reacted [35].

In this work, EOVS was synthesized by OVS and the chemical structure was characterized by Fourier transform infrared (FTIR) spectra, ^{1}H nuclear magnetic resonance (NMR) spectra and XPS. Then a series of flame-retardant EP composites containing PAPP and EOVS were prepared. The thermal stability of EP/PAPP/EOVS composites was tested with thermal gravimetric analysis (TGA). Besides, the flame retardancy and mechanical properties of the EP composites were both analyzed comprehensively. Furthermore, the flame-retardant mechanism of PAPP/EOVS flame retardants was explored by SEM, EDS, LRS, XPS and TG-FTIR.

2. Experimental

2.1. Materials

Diglycidyl ether of bisphenol A (DGEBA, epoxide equivalent weight: 185 g/eq) was provided by Guangdong Tongyu Advanced Materials Co., Ltd., China. Piperazine pyrophosphate (PAPP) was supplied by Jiangsu JITRI Advanced Polymer Material Research Institute Co., Ltd., China. Octavinyl silsesquioxane (OVS, 98%) was purchased from Zhengzhou Alpha Co., Ltd., China. 4,4′-Diaminodiphenyl methane (DDM), acetic acid, concentrated sulfuric acid, trichloromethane, hydrogen peroxide and sodium carbonate were purchased from Chengdu Chron Chemicals Co., Ltd., China.

2.2. Synthesis of EOVS

OVS (5 g) and trichloromethane (80 ml) were added into a 250 ml three-neck round bottom flask and stirred. When the system was completely dissolved, acetic acid (40 ml) and concentrated sulfuric acid (2 ml) were added. The temperature was raised to 70 °C with electromagnetic mechanical stirring, and hydrogen peroxide (80 ml) was slowly added dropwise. The reaction was condensed and refluxed for 6 h, then the reaction solution was washed with sodium carbonate and deionized water. Finally, the solution was vacuum dried to remove the water phase and obtained the EOVS. The synthetic route was shown in Scheme 1.

Table 1
The formulation of flame-retardant EP composites.

Samples	Epoxy resin (g)	DDM (g)	Flame retardants (g)	
			PAPP	EOVS
EP	100.0	26.8	0	0
EP1	90.0	26.8	10.0	0
EP2	90.0	26.8	9.5	0.5
EP3	90.0	26.8	9.0	1.0
EP4	90.0	26.8	8.0	2.0

2.3. Preparation of flame-retardant EP materials

Firstly, PAPP, EOVS and DGEBA were added into a single neck flask according to Table 1. The mixture was stirred mechanically and mixed at 90 °C for 6 h. Thereafter, the equivalent of curing agent DDM were added into the flask with stirring lasted for 20 min. Then the homogeneous mixture was transferred quickly to a preheated mold and cured according a programmed temperature of 105 °C for 2 h, 150 °C for 2 h. Finally, the cured materials were successfully prepared and respectively named as EP1, EP2, EP3 and EP4. The mass ratio calculation of flame retardants didn't include the weight of DDM, for example the EP1 includes 10 wt% PAPP. Besides, EP was also prepared through the above production process except the first step.

2.4. Characterization

FTIR spectra were recorded with a Nicolet 6700 infrared spectrometer (Thermo Fisher Scientific, Waltham, Massachusetts, USA) with KBr tablet method and the range of wavenumber is from 4000 to 500 cm^{-1}.

^{1}H NMR spectra were analyzed by an Avance II-400 MHz NMR spectrometer. Deuterated dimethyl sulfoxide (DMO-d6) was used as the test solvent.

XPS was analyzed by an AXIS UTLTRA DLD Multifunctional X-ray Photoelectron Spectrometer (Shimadzu/Kratos Ltd., Manchester, UK) with the excitation at 1486.8 eV from an Al K alpha.

TGA was measured with TA Q50 (TA Instruments Co. Ltd., New Castle, DE, USA) at a heating rate of 10 °C/s from 50 to 700 °C under nitrogen flow rate of 50 mL/min.

The LOI tests were performed on a JF-3 LOI instrument (Nanjing Jiangning Analytical Instrument Co., Ltd.) according to ASTM D 2863-77, and the size of the samples was 100 × 10 × 4 mm^3. According to GB/T 2408-2008, the UL-94 tests were analyzed by a vertical flame tester (Dongguan Jinte Instrument Co., Ltd.) and the size of samples was 125.0 × 13.0 × 3.2 mm^3.

CC tests were analyzed by an FTT-0476 cone calorimeter (UK) at an external heat flux of 50 kW/m^2 according to ISO 5660 with the size of 100 × 100 × 4 mm^3.

The surface morphology of char residues after combustion were characterized by a SEM (JSM-5900LV, JEOL. Ltd., Tokyo, Japan) at an accelerating voltage of 10 kV. EDS (INCA, Oxford Instrument) was used to investigate the surface elemental content of char residue.

LRS test was performed on a Laser Raman spectrometer (RenishawinVia, Renishaw) with excitation at 530 nm from an argon laser and a scanning range of 3000 to 500 cm^{-1} to investigate the char residues.

TG-FTIR test was conducted on a TG 209 F3 thermal analyzer (Netzsch, Germany) coupled with an FTIR spectrometer (Thermmo Fisher Scientific, US) through a heated transfer line maintained at 250 °C. The sample about 6–8 mg was heated from 50 to 700 °C at a heating rate of 10 °C/min under a nitrogen flow rate of 40 ml/min.

Dynamic mechanical analysis (DMA) was measured with TA DMA Q800 (USA) from 50 to 250 °C with the heating rate of 3 °C/min in a three-point bending mode and a frequency of 1 Hz.

The tensile strength was tested with a DWD-10KN mechanical performance testing machine (Sichuan, CHN). The impact strength was measured with a JYM 17XJJ-50 impact tester with the size of 80 × 10 ×

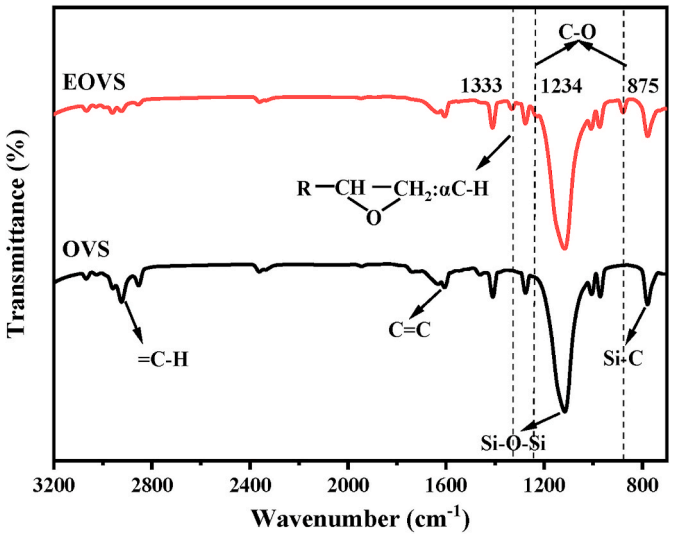

Fig. 1. FTIR spectra of OVS and EOVS.

4 mm^3.

3. Results and discussion

3.1. Characterization of EOVS

FTIR spectra of OVS and EOVS are shown in Fig. 1. In the spectra of OVS and EOVS, several similar characteristic peaks are observed. The absorption peak around 1118 cm^{-1} is due to the stretching vibration of Si-O-Si; the peak at 778 cm^{-1} is ascribed to the stretching vibration of Si-C; the absorption peak at 1605 cm^{-1} belongs to C═C; the peak at 2928 cm^{-1} is due to the stretching vibration of = C-H. In the spectrum of EOVS, the new peaks at 875 cm^{-1} and 1234 cm^{-1} are attributed to the stretching vibration of C-O-C, and the peak at 1333 cm^{-1} belongs to the bending vibration of oxirane group's C-H, indicating the existence of epoxy groups in EOVS. Moreover, the intensity of the C═C and = C-H absorption peaks decreases in the spectra of EOVS. These differences prove that the OVS is successfully converted into EOVS.

In addition, the ^{1}H NMR spectra were adopted to analyze the chemical structure of OVS and EOVS. As presented in Fig. 2, the OVS and EOVS have similar chemical shifts at 5.9–6.1 ppm which belong to the αH and βH of vinyl. For EOVS, there are another three shifts at 2.26, 2.79 and 2.92 ppm which attribute to the hydrogen of oxirane group. The chemical structure of EOVS was further investigated by XPS. As shown in Fig. 3, the C_{1s} spectrum has the characteristic peak at 286.05 eV (C-O and C═C groups) and the O_{1s} spectrum has the characteristic peak at 533.2 eV (C-O groups), further proving the existence of epoxy groups in EOVS. These results confirm that the EOVS was successfully synthesized by OVS.

3.2. Thermal stability

TGA was applied to investigate the thermal decomposition behavior and thermal stability of PAPP, EOVS, EP and EP composites under nitrogen atmosphere, the curves of TGA and DTG are shown in Fig. 4. And the relevant data are listed in Table 2, including the temperature at the 5 wt% weight losses ($T_{5\%}$), the temperature at the maximum weight loss rate (T_{max}), the maximum weight loss rate (MLR_{max}) and the residual weight at 700 °C (R_{700}).

As presented in Fig. 4a and b, the $T_{5\%}$ of EOVS and PAPP are 271.6 °C and 323.3 °C, respectively. Compared with EOVS and PAPP, EP has higher $T_{5\%}$ (360.8 °C), that is the reason why EP composites decompose earlier that EP. EP has only one decomposition stage at 344–518 °C under nitrogen atmosphere. But the decomposition of PAPP can be divided into three stages. The first stage is located at 270–320 °C, mainly attributes to the release of H_2O due to the existence of -OH·NH- [20,36]. The temperature of the second stage is at 320–440 °C, which is a complicated decomposition process that the char started to form catalyzed by phosphoric acid and its derivatives [36]. The third stage occurs between 440 and 700 °C, corresponding to the further decomposition of the formed char. The thermal decomposition process of EOVS has only one stage locating at 230–330 °C, attributing to the formation of silicon dioxide (SiO_2) and silicon carbide (SiC) [35,37,38]. Compared with the R_{700} of EP (13.0%), both PAPP and EOVS show a high stability with 27.2% and 27.3% residual weight at 700 °C, respectively.

As shown in Fig. 4c and d, the $T_{5\%}$ and T_{max} of pure EP are 360.8 °C and 373.3 °C, respectively. With the introduction of 10 wt% PAPP, the $T_{5\%}$ and T_{max} of EP1 reduce to 344.1 °C and 353.1 °C. Compared with EP and EP1, the $T_{5\%}$ and T_{max} of EP2 distinctly reduce to 331.1 °C and 348.6 °C, which attributes to the early decomposition of PAPP and EOVS. The MLR_{max} of EP composites show a slight decline compared with EP. In addition, the MLR_{max} of EP1 is lowest among all EP composites, this is because the MLR_{max} of PAPP is only 0.37%/°C and the addition of PAPP will decrease the MLR_{max} of EP composites. It can be observed that the R_{700} of EP3 is 27.3%, much higher than that of EP (13.0%) and EP1 (20.7%), indicating the incorporation of PAPP and EOVS promote the charring ability of EP composites.

3.3. Flame retardancy

3.3.1. LOI and UL-94 tests

The LOI and UL-94 tests were performed to characterize the flame retardancy of EP and EP composites, and the results are summarized in Table 3. It can be seen that pure EP only displays a LOI value of 25.4%. The existence of PAPP makes the LOI value of EP1 reach 28.8% and the UL-94 level pass V-1 rating. With the incorporation of PAPP and EOVS, the flame retardancy of EP composites is obviously enhanced. The LOI value of EP3 increases to 32.4% and it reaches V-0 rating in UL-94 test.

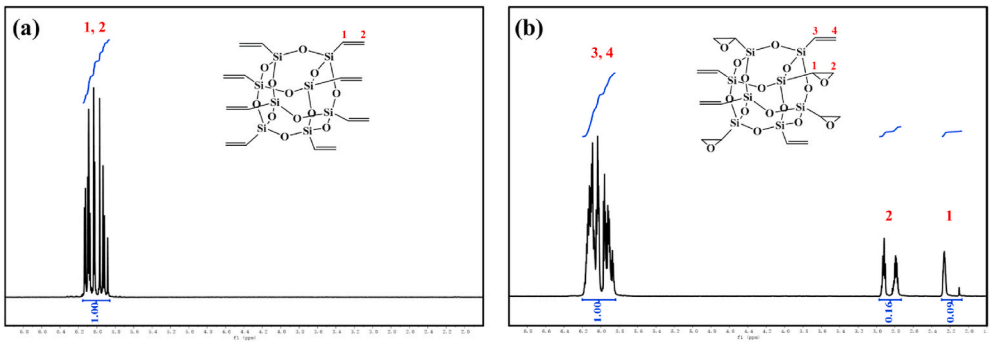

Fig. 2. ^{1}H NMR spectra of OVS and EOVS.

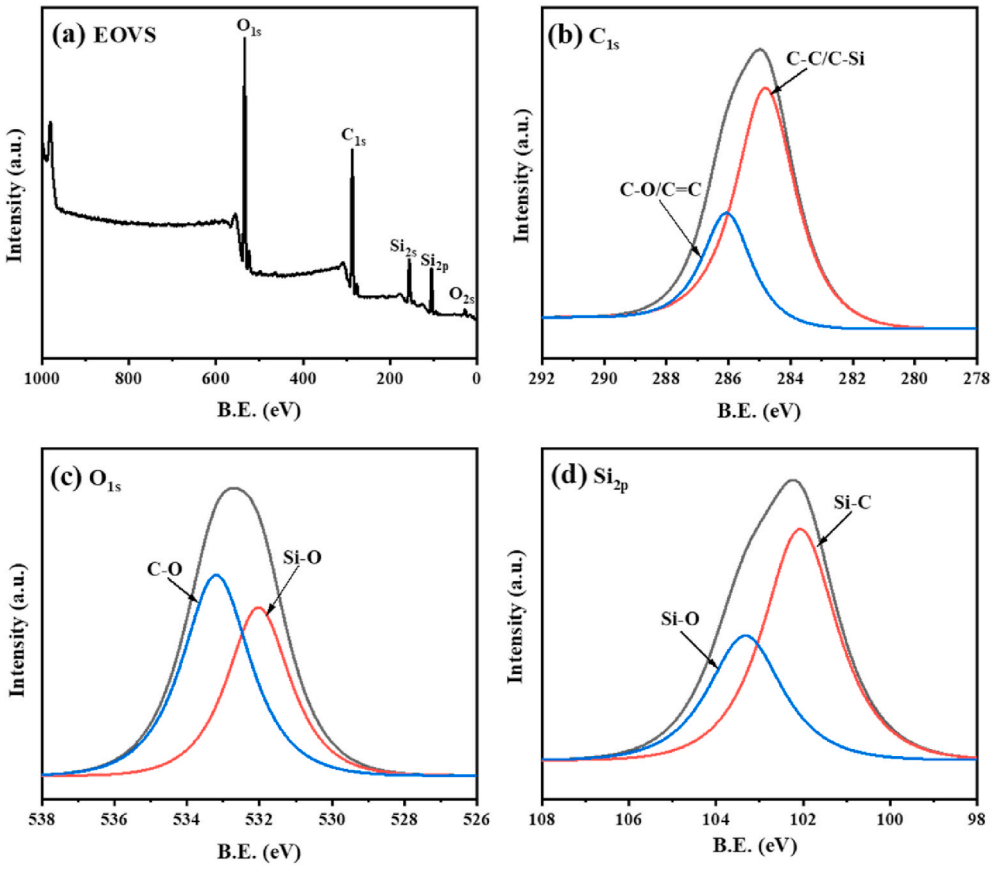

Fig. 3. XPS spectra of EOVS.

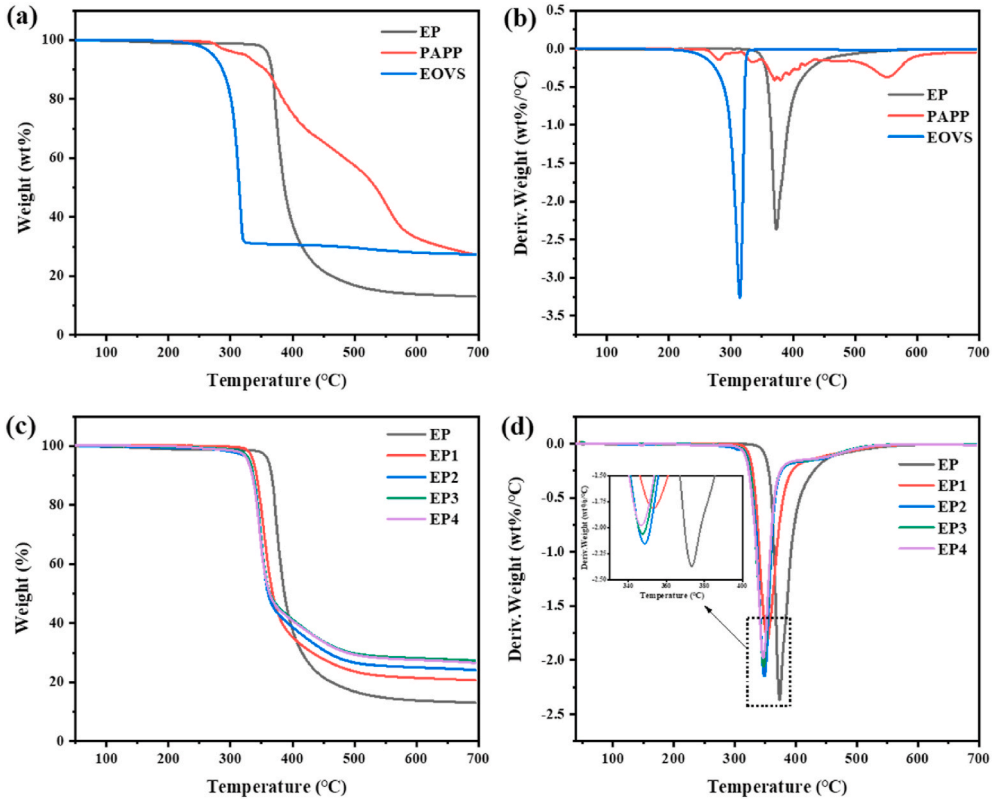

Fig. 4. TG and DTG curves of PAPP, EOVS, EP and EP composites.

Table 2
Thermogravimetric data of PAPP, EOVS, EP and EP composites.

Samples	$T_{5\%}$ (°C)	T_{max} (°C)	MLR_{max} (%/°C)	R_{700} (%)
PAPP	323.3	552.2	0.37	27.2
EOVS	271.6	314.4	3.26	27.3
EP	360.8	373.3	2.34	13.0
EP1	344.1	353.1	1.81	20.7
EP2	331.1	348.6	2.15	24.1
EP3	330.7	347.4	2.06	27.3
EP4	327.8	346.7	1.98	26.5

Table 3
LOI and UL-94 tests results of EP and EP composites.

Samples	LOI (%)	UL-94 test		
		t_1/t_2 [a] (s)	Dripping	Rating
EP	25.4	No self-extinction	YES	NR
EP1	28.8	31.04/11.56	No	V-2
EP2	31.5	5.27/16.05	No	V-1
EP3	32.4	4.38/7.41	No	V-0
EP4	31.8	24.84/18.64	No	V-1

[a] average afterflame time after the first/second 10 s ignition.

As shown in Fig. 5, the EP is easy to ignite and has no self-extinguishing. On the contrary, the EP3 exhibits excellent self-extinguishing during veridical combustion, thus EP3 is selected for the following tests.

3.3.2. Cone calorimeter tests

To further investigate the combustion performance of EP and EP composites, the results of cone calorimeter tests in terms of HRR, THR, SPR and TSP curves for EP and EP composites are shown in Fig. 6. And several significant parameters, such as the PHRR, THR, PSPR, TSP, time to ignition (TTI), average effective heat combustion (av-EHC), average carbon oxide yield (av-COY) and average carbon dioxide yield (av-CO_2Y) are summarized in Table 4.

It is obvious that the EP composites are easy to be ignited in the presence of PAPP and EOVS. As shown in Table 4, the TTI for EP, EP1 and EP3 are 76 s, 45 s and 39 s, respectively. During the combustion process of the materials, the early decomposition of PAPP and EOVS will catalyze the decomposition of EP, resulting in weak ignition resistance for EP composites.

HRR is one of the most important parameters to characterize combustion intensity, combining HRR and THR can better evaluate the combustion behavior of materials. Fig. 6a and b show that pure EP burns with a sharp PHRR peak of 1320 kW/m^2 and a high THR value of 91.1 MJ/m^2 with the residue of 13.9% remained, existing a potential risk of thermal and fire hazards. Compared with the high PHRR and THR values of pure EP, EP1 shows remarkable PHRR reduction of 46% and THR reduction of 15%. Besides, the residue of EP1 is 24.1%. With the introduction of 9 wt% PAPP and 1 wt% EOVS, EP3 has the minimum PHRR and THR values in all samples, which are respectively reduced by 81% and 25% compared with those of EP. Meanwhile, the residue of EP3 reaches 31.5%, which are mainly due to the barrier effect of the char layer. It can be speculated that the incorporation of EOVS and PAPP promotes the formation of the carbon layer, which can not only inhibit the transfer of heat and oxygen but protect underlying materials, finally leading to the decrease of the PHRR and THR values.

Av-EHC reveals the combustion extent of volatile gases, which can be used to investigate the flame-retardant mechanism in the gas phase. In Table 4, the value of EP1 (21.5 MJ/kg) are slightly reduced compared with pure EP (22.4 MJ/kg), proving the presence of a gas phase flame-retardant effect. The reason for this phenomenon is speculated to be that the PAPP releases some noncombustible gases which can dilute the concentration of combustible gases, and produces some phosphorus-containing compounds which have a flame inhibition effect in the gas phase [36,39,40], resulting in a slight decrease of av-EHC value. The av-EHC value of EP1 is close to the value of EP3 (21.4 MJ/kg), indicating that the PAPP/EOVS flame retardants mainly paly the synergistic flame-retardant effect in the condensed phase.

Subsequently, av-COY and av-CO_2Y can also offer som [41]e objective evidence about flame-retardant mechanism. An increase of av-COY value and a decrease of av-CO_2Y value is attributed to the suppressed oxidation process in the gas phase [41]. Table 4 shows the increase of av-COY value is ordered EP □ EP3 □ EP1, and the increase of av-CO2Y value is ordered EP1 □ EP3 □ EP. EP1 has the largest av-COY value and the smallest av-CO2Y value in all samples, indicating that more incomplete combustion product (CO) and less complete combustion product (CO_2) are produced during combustion. The suppressed

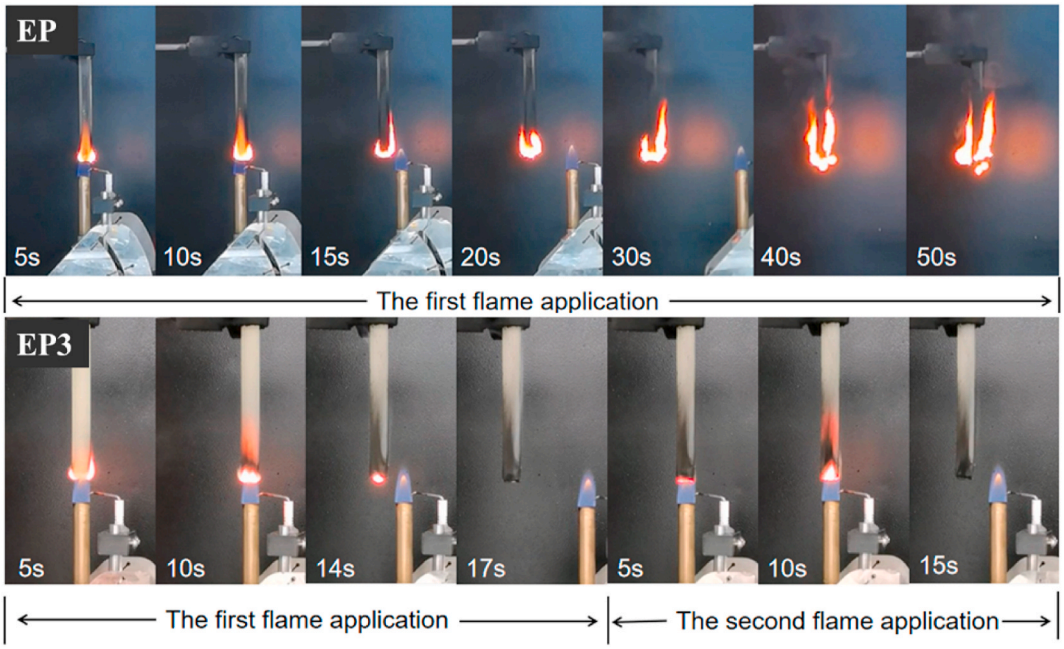

Fig. 5. Photographs of EP and EP3 with different ignition time during veridical combustion (Timing when flame is applied to the sample).

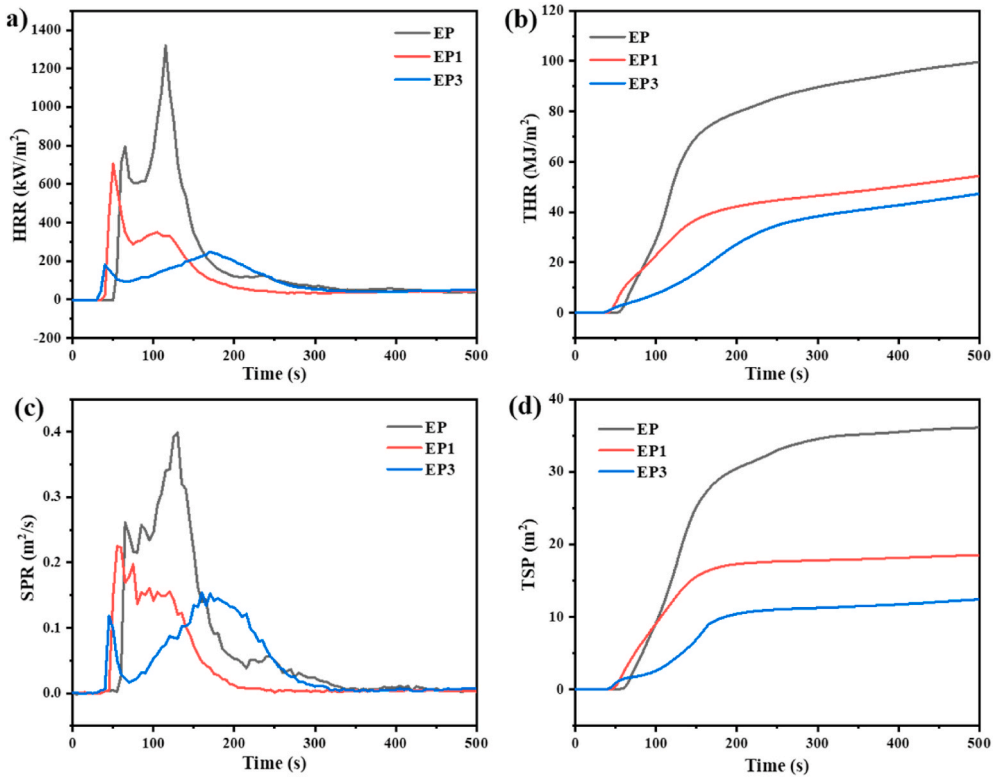

Fig. 6. Cone calorimetric data of EP, EP1 and EP3: (a) HRR, (b) THR, (c) SPR, (d) TSP.

Table 4
Cone calorimetric test results of EP and EP composites.

Samples	TTI (s)	PHRR (kW/m^2)	THR (MJ/m^2)	Residues (%)	av-EHC (MJ/kg)	av-COY (kg/kg)	av-CO_2Y (kg/kg)	PSPR (m^2/s)	TSP (m^2)
EP	76 ± 1	1320 ± 15	91.1 ± 1.4	13.9 ± 0.9	22.4 ± 0.4	0.09 ± 0.02	1.76 ± 0.04	0.40 ± 0.02	36.5 ± 0.5
EP1	45 ± 2	707 ± 17	77.5 ± 2.2	24.1 ± 0.5	21.5 ± 0.2	0.13 ± 0.02	1.50 ± 0.03	0.22 ± 0.03	19.7 ± 0.6
EP3	39 ± 1	248 ± 16	68.4 ± 1.6	31.5 ± 0.6	21.4 ± 0.3	0.11 ± 0.03	1.54 ± 0.03	0.15 ± 0.02	15.8 ± 0.4

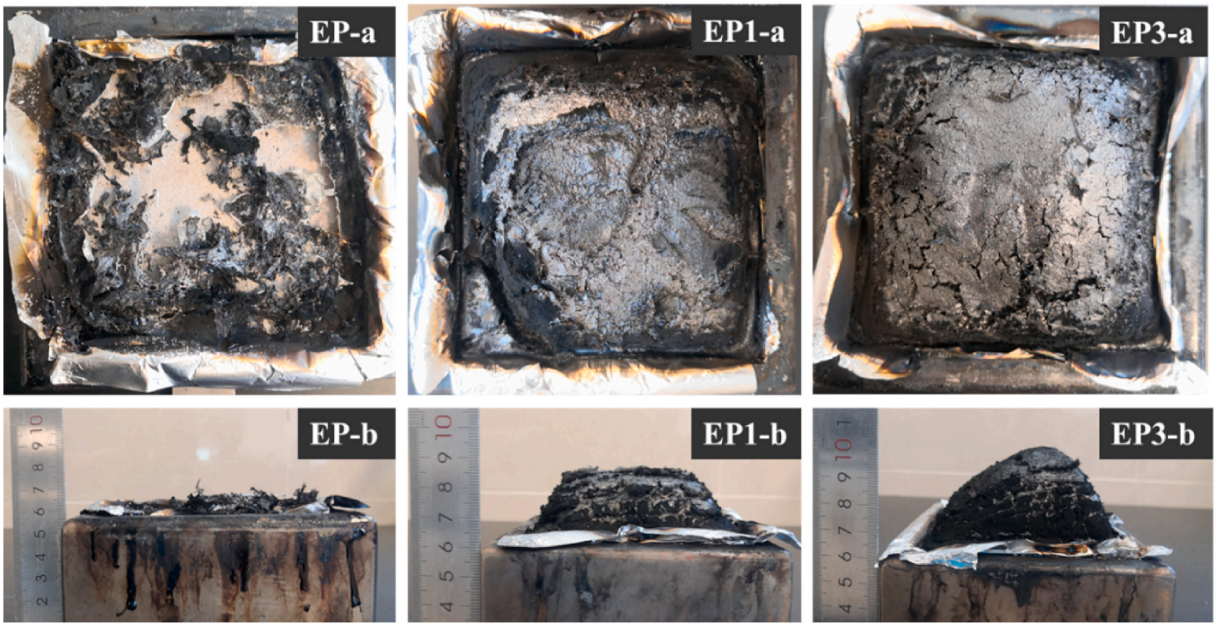

Fig. 7. Digital photos of the char residues for EP (a), EP1 (b) and EP3 (c).

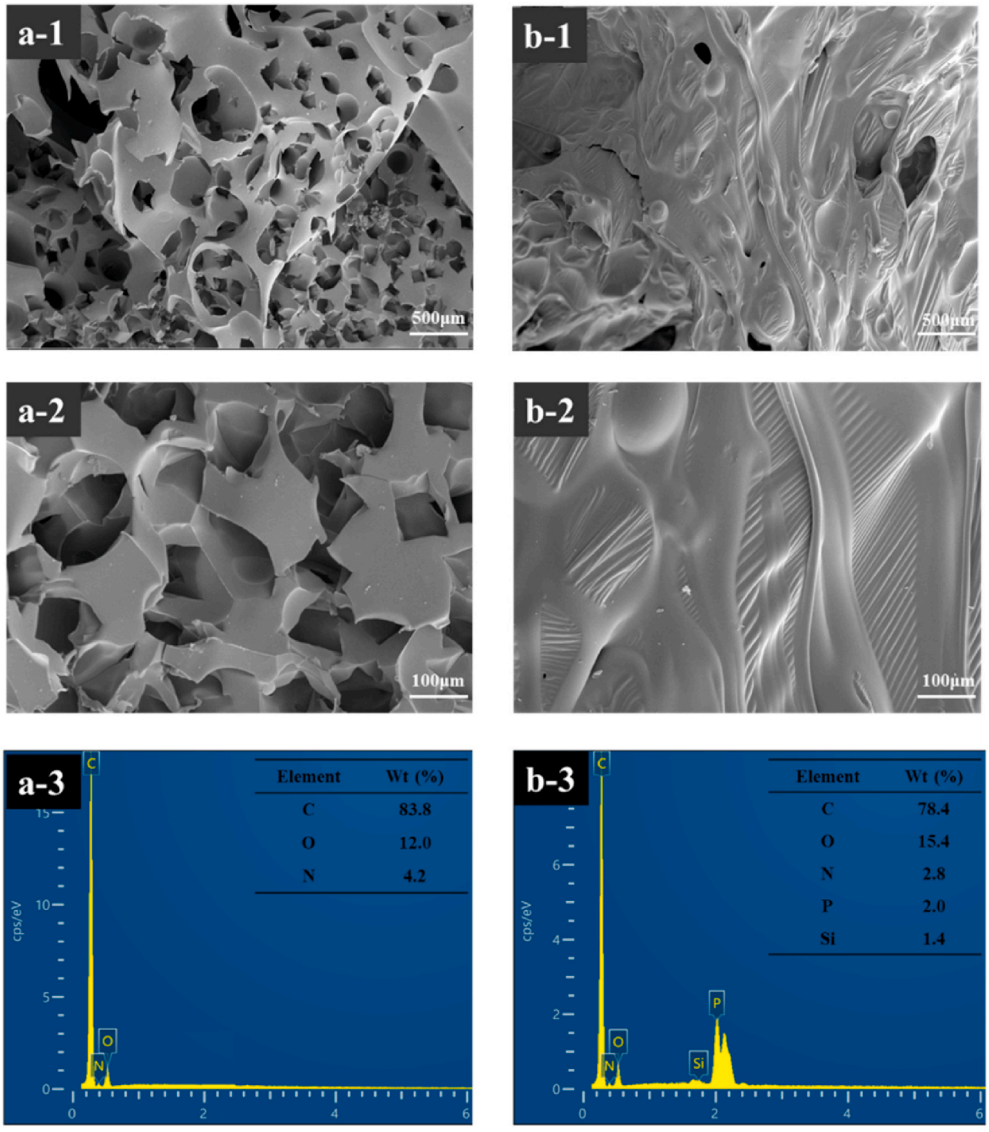

Fig. 8. SEM images and EDS pictures of the char residues for EP (a) and EP3 (b).

oxidation process of EP1 is stronger than other samples, mainly owing to the phosphorus flame inhibition action in the gas phase. Besides, the smoke production capacity of the material is one of the important factors to evaluate the fire risk. By means of Fig. 6c and d, it can be observed that PAPP and EOVS can effectively reduce the smoke release of the EP. The PSPR and TSP values of pure EP are 0.40 m^2/s and 36.5 m^2, respectively. Compared with EP, the PSPR and TSP values of EP1 are respectively reduced by 45% and 46%, and EP3 are respectively reduced by 63% and 57%. It can be inferred that the incorporation of PAPP and EOVS promotes the formation of a dense carbon layer which insulates the diffusion of combustible volatiles into flame zone and reduces the transmission efficiency of gases, endowing the EP composites with excellent smoke suppression.

3.4. Flame-retardant mechanism

According to the above results, it is speculated that PAPP and EOVS improve the flame retardancy of EP by exerting synergistic flame-retardant effect in combustion. In this part, the char residues after combustion were observed and characterized by SEM, EDS, LRS and XPS, and the volatile products were analyzed by TG-FTIR.

3.4.1. Char residues analysis

Fig. 7 shows the digital photos of the char residues of EP, EP1 and EP3 after cone colorimeter tests. As seen, the burned pure EP form a broken char layer which appears large cracks and holes. On the contrary, the char layer of EP3 seems robust and compact. What's more, the amount of char residues for EP3 is obviously increased. The small cracks of EP3 on the surface are probably caused by the pyrolysis gas releasing from the combustion matrix. As for EP1, the char layer isn't as thick as EP3 and seems fluffier. To better observe the char layer micro-morphology, SEM and EDS tests results are shown in Fig. 8. In the SEM images of pure EP, a loose porous surface can be clearly observed. With the introduction of PAPP and EOVS, the surface of char residue becomes dense and compact. The results of EDS demonstrate that the char residue of EP has three elements: C, O and N, while EP3 includes five elements: C, O, N, P and Si. The mass fraction of N in the char residue of EP is 4.2%, but this of EP3 is 2.8%. The reduction of N content indicates that the EP3 may decompose into some nitrogen-containing gases during combustion. The presence of silicon element can infer that the decomposition of EOVS produced substances such as SiO_2 and SiC existing in the carbon layer [35]. The lower content of phosphorus element of char layer indicates that one part of the phosphorus compounds may decompose into phosphoric acid and other phosphorus

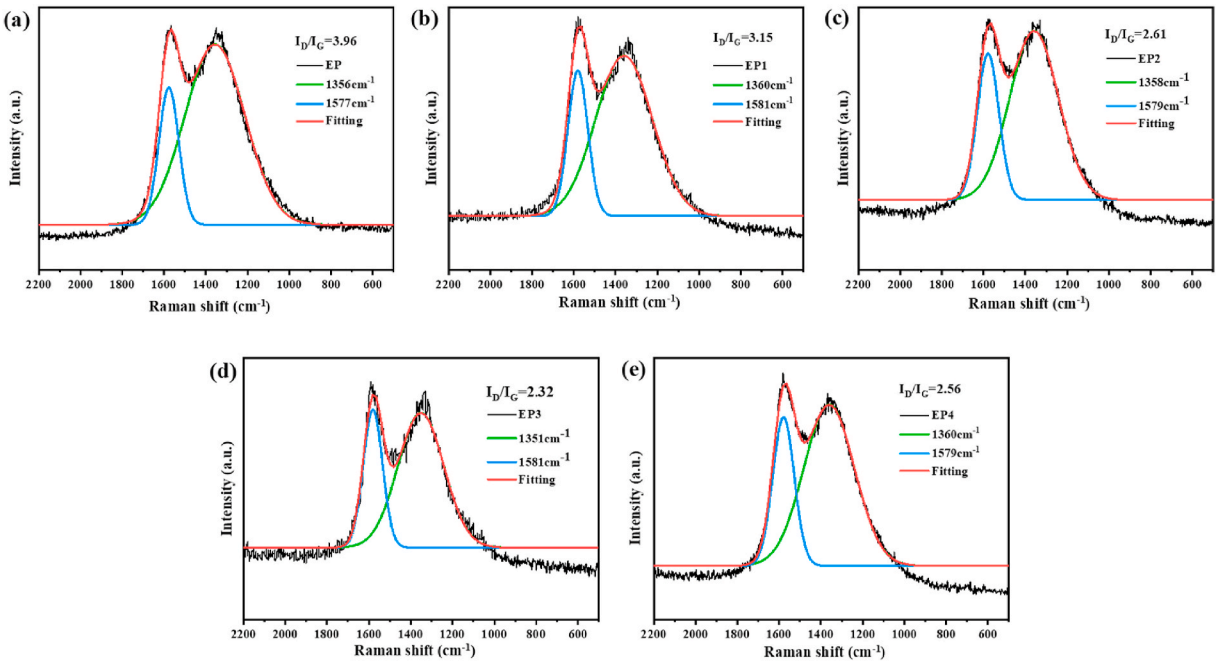

Fig. 9. Raman spectra of the char residues for (a) EP, (b) EP1, (c) EP2, (d) EP3 and (e) EP4.

derivatives, which can catalyze the dehydration and cross-linking on the surface of matrix and promote the formation of a dense carbon layer. And other part of phosphorus compounds may be decomposed into gaseous phosphorous compounds, which exert flame inhibition effect in the gas phase [41–43].

Fig. 9 provides the Raman spectra of the char residues for EP and EP composites. All the spectra distinguish into two broad peaks at approximately about 1358 cm^{-1} and 1580 cm^{-1}, corresponding to the D and G band, respectively. The D band is associated with the disorder of the sp^2 structure of graphene sheets, and the G band is related to the in-plane tangential stretches of C-C bonds in organized graphitic structure [44]. The intensity ratio of D band and G band (I_D/I_G) is widely used to characterize the graphitization degree of char residue structure [45]. The smaller value of I_D/I_G represents the less disordered structure, which also means the higher graphitization degree. According to Fig. 9, the I_D/I_G values follow the sequence of EP (3.96) □EP1 (3.15) □EP2 (2.61) □ EP4 (2.56) □EP3 (2.32). The results of Raman spectrum reveal that the char residue of EP3 is composed of graphite-like complexes. The dense and compact graphite-like complexes inhibit the transfer of heat and gas, and also offer better protection for inner composites. The Raman spectra of char residues are consistent with the results of SEM.

To further confirm the decomposition products of EP composites in the condensed phase, the char residues for EP and EP3 were characterized by XPS. As presented in Fig. 10a and b, the C_{1s} spectra of char residues for EP and EP3 both have the peaks at 284.6 eV (C-C and C-Si groups), 285.75 eV (C-O and C-N groups) and 289.3 eV (C═O group). What's more, in the C_{1s} spectrum of char residue for EP3, the intensity of peak at 285.75 eV is significantly enhanced due to the existence of C═C group, proving the form of aromatic structure in char residue. The O_{1s} spectra are shown in Fig. 10c and d, EP3 has three characteristic peaks at 531.65 eV (C═O and P═O groups), 533 eV (C-O and P-O groups) and 534.1 eV (Si-O group). The presence of P═O and P-O groups reveals the existence of phosphate groups. And the existence of Si-O group indicates EOVS decomposes into siloxane existing in the carbon layer. Fig. 10e and f present the N_{1s} spectra, the char residues of EP and EP3 both have two similar peaks at 398.85 eV (N-H group) and 400.15 eV (C-N group). The result proves the existence of C-N structure in the char residue. After the introduction of PAPP, there appears a new peak at 401.45 eV (N-O group) in the N_{1s} spectrum of char residue for EP3. Fig. 10g and h show the P_{2p} and Si_{2p} spectra of the char residue for EP3, respectively. The characteristic peaks are ascribed to 133.8 eV (P-O group), 134.95 eV (P═O group), 102.2 eV (Si-C group) and 103.5 eV (Si-O group), which further prove the existence of phosphorous compounds, SiC and SiO_2 in the carbon residue. Based on the above results, it can be inferred that the PAPP and EOVS are beneficial for enhancing charring ability and improving the char layer morphology.

3.4.2. *Evolved gas analysis*

TG-FTIR spectroscopy was adopted to investigate gaseous products during thermal decomposition. As can be seen from Fig. 11a, when the temperature reaches 236 °C, absorption peaks assigned to phenol derivatives (3844 and 3658 cm^{-1}), CO_2 (2408-2258 cm^{-1}), CO (2183 and 2116 cm^{-1}) and aromatic compounds (1692-1530 cm^{-1}) are observed. At 396 °C, all the peaks become stronger and no new peaks appeare, indicating that the decompositon of pure EP involves only one process, this resluts is consistent with the TGA test. Note that some peaks are stilled observed at 694 °C, confirming the continuous decomposition of pure EP.

As shown in Fig. 11b, the decompostion process of EP3 is different from that of EP. At 396 °C, absorption peaks belonged to phenol derivatives (3782 and 3651 cm^{-1}), aromatic compounds (3148-2864 cm^{-1}), and carbonyl compounds (1735 cm^{-1}) are observed. Besides, there appears a strong peak attributed to H_2O (3551 cm^{-1}), which is due to the dehydration of PAPP, this result is accorded with the TGA of PAPP. At 484 °C, the peaks of H_2O and carbonyl compounds weaken. And some new peaks emerge, including CO (2190 and 2102 cm^{-1}), NH_3 (1004-901 cm^{-1}), Si-O (1184 cm^{-1}), P-C_{Ar} (1591, 1489 and 776 cm^{-1}), P═O (1257 cm^{-1}) and P-O (832 cm^{-1}). The PAPP contributes to the production of H_2O and NH_3, which can reduce the concentration of combustible gases to achieve dilution in the gas phase. What's more, a strong characteristic peak of CO appears at 484 °C, which is attributed to the suppressed oxidation process caused by phosphorous compounds in the gas phase. When the temperature rises from 484 to 694 °C, many characteristic peaks weaken until they disappear. It can be drawn that the pyrolysis products for EP at the beginning are mainly composed of H_2O, carbonyl compounds, etc. With the increase of temperature, CO, NH_3, phosphorous compounds and other gases are released.

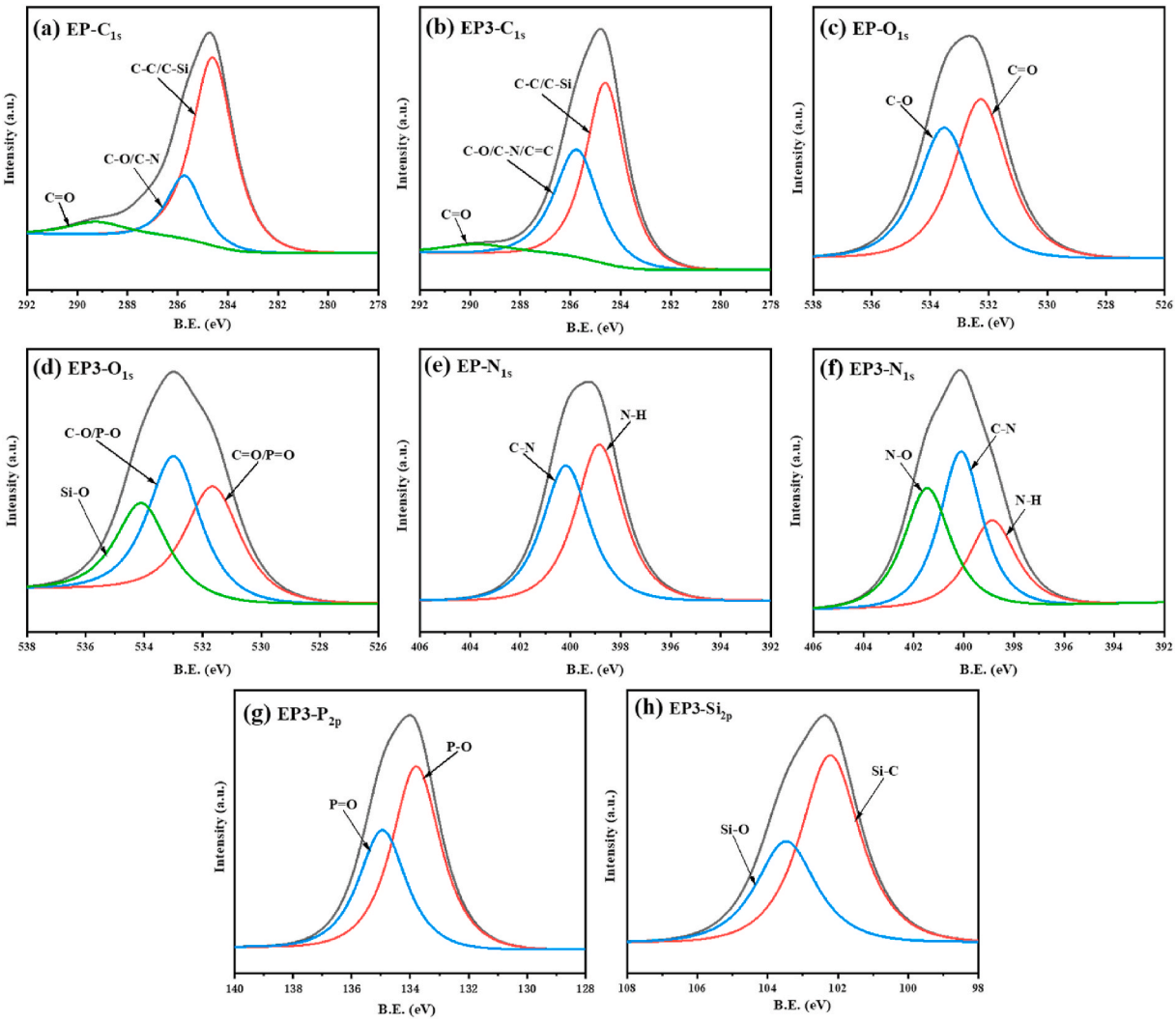

Fig. 10. XPS results of char residues for EP and EP3.

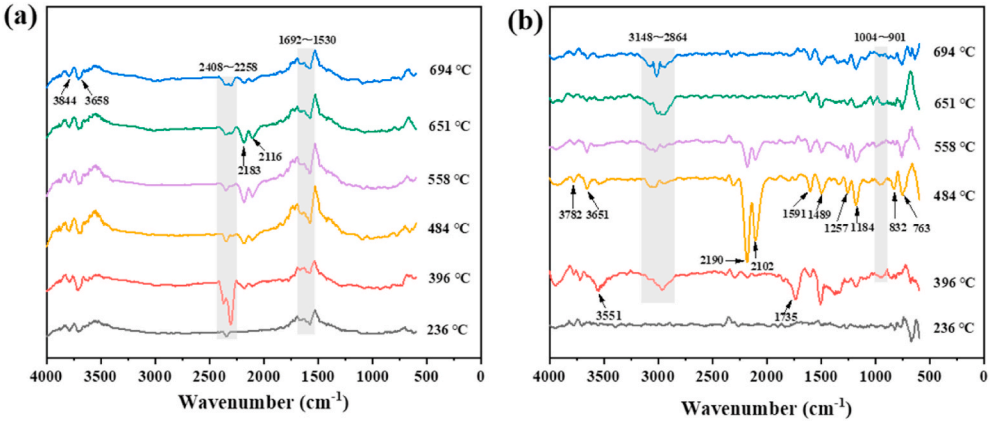

Fig. 11. FTIR spectra of volatilization products for EP (a) and EP3 (b) at various temperatures.

3.4.3. *Flame retardant mechanism analysis*

Based on the above discussions, the possible flame-retardant mechanism of PAPP/EOVS flame retardants in EP is proposed in Fig. 12 [46] and schematic illustration of flame-retardant mechanism is shown in Fig. 13. In the condensed phase, PAPP decomposes into phosphoric acid and other phosphorus-containing derivatives, which accelerate the dehydration of epoxy resin and cause cyclization or crosslinking of the matrix surface. At the same time, EOVS decomposes into silicon-containing compounds such as SiO_2 and SiC. Due to the low surface energy of silicon oxide, it will migrate to the surface of the matrix and form a dense and stable carbon layer. Furthermore, with the production of a large amount of pyrolysis gases the char layer expands

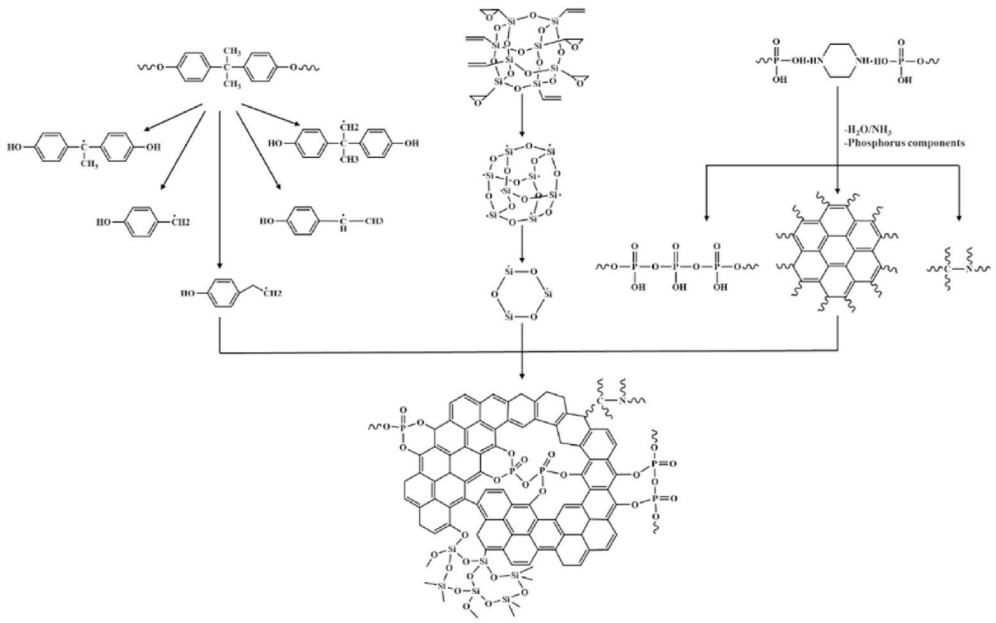

Fig. 12. Possible flame-retardant mechanism of PAPP/EOVS flame retardants.

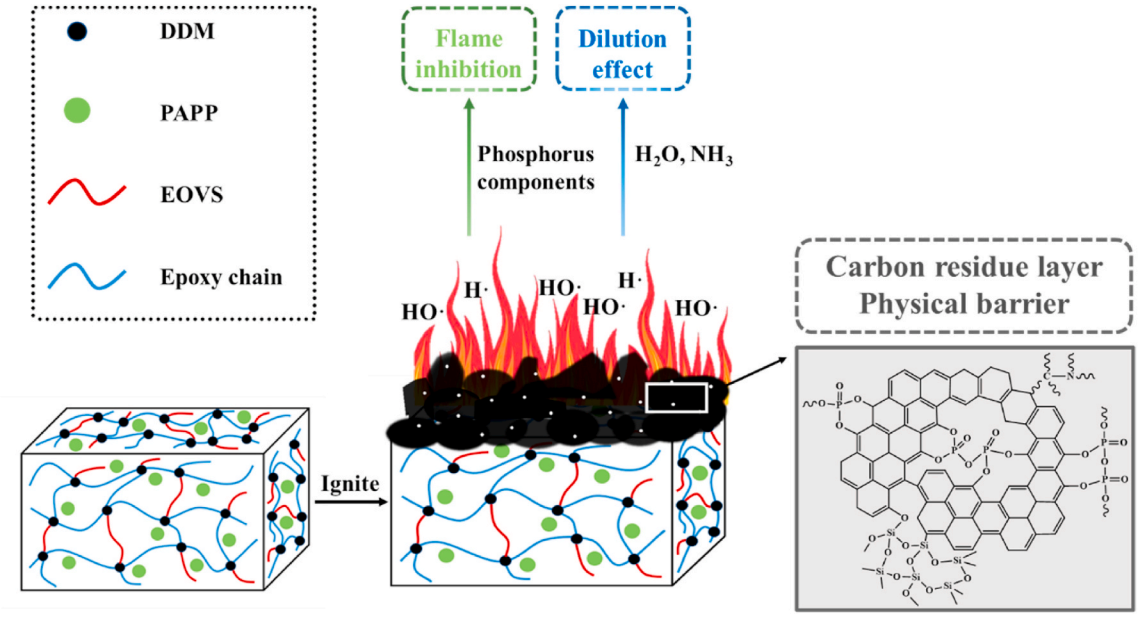

Fig. 13. Schematic illustration of flame-retardant mechanism.

and forms a physical barrier, which plays a dominant role in enhancing the flame retardancy of EP composites. In the gas phase, the released non-combustible gases such as H_2O and NH_3 can not only promote the expansion of the carbon layer but dilute the combustible gases concentration. Simultaneously, the gaseous phosphorous compounds can act as flame inhibitors to suppress the burning process.

3.5. Mechanical properties

DMA was applied to characterize the dynamic mechanical behavior of EP and EP composites, storage modulus (E') and loss tangent (tan δ) versus temperature curves are shown in Fig. 14 and the relevant data are presented in Table 5. The peak of tan δ is defined as glass transition temperature (Tg) [47–49]. It can be obviously observed that the Tg value of pure EP is 168.9 °C, while values of other EP composites raised slightly. This phenomenon is due to the introduction of epoxy groups in EOVS which increases the cross-linking density of the composites, causing the increase of intermolecular binding energy, finally resulting in the increase of Tg. In addition, the intermolecular force increases with the introduction of hydroxyl groups on PAPP, also leading to the increase of Tg. As presented in Fig. 14 a, all EP materials exhibit the "rubbery plateau" after their Tg [47]. When EOVS is added, the rubbery state modulus is obviously improved illustrating the higher cross-linking density of EP/PAPP/EOVS composites.

Tensile and impact tests were used to characterize the mechanical properties of samples, the relevant data are listed in Table 5. EP3 exhibits higher tensile strength (58.2 MPa) and impact strength (11.3 kJ/m^2) than pure EP (47.2 MPa, 9.4 kJ/m^2). But the tensile and impact strength of EP4 only reaches 45.2 (MPa) and 7.5 (kJ/m^2). And the tensile strength and impact strength of EP composites first increase and

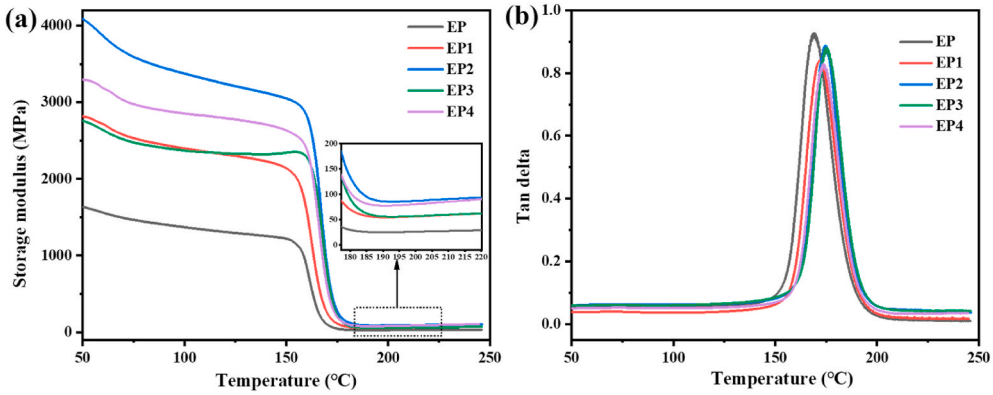

Fig. 14. DMA curves of EP and EP composites.

Table 5
Mechanical properties test results of EP and EP composites.

Samples	Tg (°C)	E′ at 50 °C (MPa)	Tensile strength (MPa)	Elongation at break (%)	Impact strength (kJ/m^2)
EP	168.9 ± 1.8	1635 ± 15	47.2 ± 1.4	6.1 ± 1.1	9.4 ± 1.1
EP1	172.1 ± 1.4	2815 ± 21	48.4 ± 2.1	6.6 ± 0.7	8.3 ± 1.4
EP2	174.7 ± 1.7	4091 ± 19	55.6 ± 1.5	7.2 ± 0.9	10.0 ± 1.3
EP3	175.7 ± 1.3	2757 ± 16	58.2 ± 1.7	7.7 ± 1.1	11.3 ± 1.3
EP4	174.1 ± 1.5	3297 ± 20	45.2 ± 2.0	5.9 ± 1.3	7.5 ± 1.5

then decrease. The above results can be explained as follows: in theory, the strength of EP thermoset is mainly dominated by the cross-linking density if there only one changeless network exists in the EP thermoset [11,47,50,51]. When an appropriate amount of EOVS is added, the cross-linking density increases which can better disperse and bear the stress. Besides, the introduction of Si-O bonds can reduce the internal stress of the epoxy resin. These factors are responsible for increasing strength. But when the content of EOVS is too high, the strength decreases due to the phase separation in the system. To sum up, the epoxy group and Si-O bond flexible structure of the PAPP/EOVS flame retardants make the mechanical properties of EP2 and EP3 outstanding.

4. Conclusions

In this paper, EOVS is successfully synthesized and a series of EP composites containing PAPP and EOVS are prepared and characterized. With the incorporation of 9 wt% PAPP and 1 wt% EOVS, EP3 passes a UL-94 V-0 rating and acquires the LOI value of 32.4%. The results of TGA show that the introduction of PAPP and EOVS reduces the temperature at the 5 wt% weight losses but increases the char residual weight at 700 °C. The cone calorimeter tests illustrate that EP3 has the lowest PHRR, THR, PSPR and TSP values, which reveal that the introduction of PAPP and EOVS enhance the flame retardancy and smoke suppression of epoxy resin. To further explore the flame-retardant mechanism of EP/PAPP/EOVS, SEM, EDS, LRS, XPS are adopted to analyze the char residues and the evolved gases are characterized by FT-IR. The results indicate that the PAPP/EOVS flame retardants form a dense and stable carbon layer through synergistic effect in the condensed phase, and suppress combustion by dilution effect and flame inhibition in the gas phase. Besides, the tensile and impact strengths of EP2 and EP3 increase because of the introduction of epoxy groups and Si-O bonds. In general, PAPP/EOVS flame retardants can bring high efficiency flame retardancy and maintain satisfactory mechanical properties for EP, which exhibits a great application potential in the field of flame-retardant epoxy resin.

Auther statement

Shansu Li: Conceptualization, Formal analysis, Project administration, Software, Visualization, Roles/Writing-original draft. Yuan Liu: Conceptualization, Data curation, Funding acquisition, Resources, Supervision, Validation, Writing-review & editing. Yuansen Liu: Article revision. Qi Wang: Writing-review & editing.

Declaration of competing interest

The authors declare that they have no known competing financial interests or personal relationships that could have appeared to influence the work reported in this paper.

Acknowledgements

This work is financially supported by the NSAF Fund (U183010085) and the Sichuan Science and Technology Project (No. 2021YFG0083).

References

[1] Kalali EN, Wang X, Wang D-Y. Functionalized layered double hydroxide-based epoxy nanocomposites with improved flame retardancy and mechanical properties. J Mater Chem 2015;3:6819–26.
[2] Battig A, Markwart JC, Wurm FR, Schartel B. Sulfur's role in the flame retardancy of thio-ether–linked hyperbranched polyphosphoesters in epoxy resins. Eur Polym J 2020;122.
[3] Wang R, Zhuo D, Weng Z, et al. A novel nanosilica/graphene oxide hybrid and its flame retarding epoxy resin with simultaneously improved mechanical, thermal conductivity, and dielectric properties. J Mater Chem 2015;3:9826–36.
[4] Wang X, Hu Y, Song L, et al. Flame retardancy and thermal degradation mechanism of epoxy resin composites based on a DOPO substituted organophosphorus oligomer. Polymer 2010;51:2435–45.
[5] Jian R-K, Ai Y-F, Xia L, et al. Organophosphorus heteroaromatic compound towards mechanically reinforced and low-flammability epoxy resin. Compos B Eng 2019;168:458–66.
[6] Fang F, Ran S, Fang Z, et al. Improved flame resistance and thermo-mechanical properties of epoxy resin nanocomposites from functionalized graphene oxide via self-assembly in water. Compos B Eng 2019;165:406–16.
[7] Chen R, Luo Z, Yu X, et al. Synthesis of chitosan-based flame retardant and its fire resistance in epoxy resin. Carbohydr Polym 2020;245:116530.
[8] Kim M, Ko H, Park S-M. Synergistic effects of amine-modified ammonium polyphosphate on curing behaviors and flame retardation properties of epoxy composites. Compos B Eng 2019;170:19–30.
[9] Dagdag O, Bachiri AE, Hamed O, et al. Dendrimeric epoxy resins based on hexachlorocyclotriphosphazene as a reactive flame retardant polymeric materials: a review. J Inorg Organomet Polym Mater 2021.
[10] Spontón M, Ronda JC, Galià M, Cádiz V. Development of flame retardant phosphorus- and silicon-containing polybenzoxazines. Polym Degrad Stabil 2009;94:145–50.
[11] Ding J, Tao Z, Zuo X, et al. Preparation and properties of halogen-free flame retardant epoxy resins with phosphorus-containing siloxanes. Polym Bull 2009;62:829–41.

[12] Lu L, Zeng Z, Qian X, et al. Thermal degradation and combustion behavior of flame-retardant epoxy resins with novel phosphorus-based flame retardants and silicon particles. Polym Bull 2018;76:3607–19.
[13] Fang F, Song P, Ran S, et al. A facile way to prepare phosphorus-nitrogen-functionalized graphene oxide for enhancing the flame retardancy of epoxy resin. Compos Commun 2018;10:97–102.
[14] Sai T, Ran S, Guo Z, et al. Transparent, highly thermostable and flame retardant polycarbonate enabled by rod-like phosphorous-containing metal complex aggregates. Chem Eng J 2021:409.
[15] Fang F, Huo S, Shen H, et al. A bio-based ionic complex with different oxidation states of phosphorus for reducing flammability and smoke release of epoxy resins. Compos Commun 2020;17:104–8.
[16] Luo Q, Sun Y, Yu B, et al. Synthesis of a novel reactive type flame retardant composed of phenophosphazine ring and maleimide for epoxy resin. Polym Degrad Stabil 2019;165:137–44.
[17] Liu Y-L, Chang G-P, Wu C-S, Chiu Y-S. Preparation and properties of high performance epoxy-silsesquioxane hybrid resins prepared using a maleimide-alkoxysilane compound as a modifier. J Polym Sci Polym Chem 2005;43:5787–98.
[18] Zhi M, Liu Q, Chen H, et al. Thermal stability and flame retardancy properties of epoxy resin modified with functionalized graphene oxide containing phosphorus and silicon elements. ACS Omega 2019;4:10975–84.
[19] Hu Z, Zhong ZQ, Gong XD. Flame retardancy, thermal properties, and combustion behaviors of intumescent flame-retardant polypropylene containing (poly) piperazine pyrophosphate and melamine polyphosphate. Polym Adv Technol 2020;31:2701–10.
[20] Xiao X, Zhai J, Chen T, et al. Flame retardant properties of polyamide 6 with piperazine pyrophosphate. Plastics, Rubber Compos 2017;46:193–9.
[21] Xiao X, Hu S, Zhai J, et al. Thermal properties and combustion behaviors of flame-retarded glass fiber-reinforced polyamide 6 with piperazine pyrophosphate and aluminum hypophosphite. J Therm Anal Calorim 2016;125:175–85.
[22] Sun Z, Hou Y, Hu Y, Hu W. Effect of additive phosphorus-nitrogen containing flame retardant on char formation and flame retardancy of epoxy resin. Mater Chem Phys 2018;214:154–64.
[23] Xu M-J, Xia S-Y, Liu C, Li B. Preparation of poly(phosphoric acid piperazine) and its application as an effective flame retardant for epoxy resin. Chin J Polym Sci 2018;36:655–64.
[24] Chen T, Xiao X, Wang J, Guo N. Fire, thermal and mechanical properties of TPE composites with systems containing piperazine pyrophosphate (PAPP), melamine phosphate (MPP) and titanium dioxide (TiO2). Plastics, Rubber Compos 2019;48:149–59.
[25] Huo S, Song P, Yu B, et al. Phosphorus-containing flame retardant epoxy thermosets: recent advances and future perspectives. Prog Polym Sci 2021:114.
[26] Huo S, Yang S, Wang J, et al. A liquid phosphaphenanthrene-derived imidazole for improved flame retardancy and smoke suppression of epoxy resin. ACS Appl Polymer Mater 2020;2:3566–75.
[27] Zeng B, Hu R, Zhou R, et al. Co-flame retarding effect of ethanolamine modified titanium-containing polyhedral oligomeric silsesquioxanes in epoxy resin. Appl Organomet Chem 2019;34.
[28] Li S, Zhao X, Liu X, et al. Cage-ladder-structure, phosphorus-containing polyhedral oligomeric silsesquinoxanes as promising reactive-type flame retardants for epoxy resin. J Appl Polym Sci 2019;136.
[29] Meenakshi KS, Kumar SA. Development of siloxane based tetraglycidyl epoxy nanocomposites for high performance applications—study of the thermo mechanical, electrical, XRD, EDS and physical properties. Silicon 2018;11:741–9.
[30] Zhai C, Xin F, Chen Y, et al. Flame retardancy of epoxy resin nanocomposite with a novel polymeric nanoflame retardant. Polym Adv Technol 2019;30:2833–45.
[31] Liu L, Zhang W, Yang R. Flame retardant epoxy composites with epoxy-containing polyhedral oligomeric silsesquioxanes. Polym Adv Technol 2020;31:2058–74.
[32] Liu B, Wang H, Guo X, et al. Effects of an organic-inorganic hybrid containing allyl benzoxazine and POSS on thermal properties and flame retardancy of epoxy resin. Polymers 2019:11.
[33] Zhang W, Li X, Li L, Yang R. Study of the synergistic effect of silicon and phosphorus on the blowing-out effect of epoxy resin composites. Polym Degrad Stabil 2012;97:1041–8.
[34] Yang S, Wang J, Huo S, et al. Synthesis of a phosphorus/nitrogen-containing compound based on maleimide and cyclotriphosphazene and its flame-retardant mechanism on epoxy resin. Polym Degrad Stabil 2016;126:9–16.
[35] Zhai C, Xin F, Cai L, et al. Flame retardancy and pyrolysis behavior of an epoxy resin composite flame-retarded by diphenylphosphinyl-POSS. Polym Eng Sci 2020;60:3024–35.
[36] Yuan Z, Wen H, Liu Y, Wang Q. Synergistic effect between piperazine pyrophosphate and melamine polyphosphate in flame retarded glass fiber reinforced polypropylene. Polym Degrad Stabil 2021:184.
[37] Wu K, Song L, Hu Y, et al. Synthesis and characterization of a functional polyhedral oligomeric silsesquioxane and its flame retardancy in epoxy resin. Prog Org Coating 2009;65:490–7.
[38] Wang X, Song L, Yang H, et al. Simultaneous reduction and surface functionalization of graphene oxide with POSS for reducing fire hazards in epoxy composites. J Mater Chem 2012;22.
[39] Bao Q, Wang B, Liu Y, et al. Epoxy resin flame retarded and toughed via flexible siloxane chain containing phosphaphenanthrene. Polym Degrad Stabil 2020:172.
[40] Zou J, Duan H, Chen Y, et al. A P/N/S-containing high-efficiency flame retardant endowing epoxy resin with excellent flame retardance, mechanical properties and heat resistance. Compos B Eng 2020:199.
[41] Huo S, Yang S, Wang J, et al. A liquid phosphorus-containing imidazole derivative as flame-retardant curing agent for epoxy resin with enhanced thermal latency, mechanical, and flame-retardant performances. J Hazard Mater 2020;386:121984.
[42] Liu J, Dai J, Wang S, et al. Facile synthesis of bio-based reactive flame retardant from vanillin and guaiacol for epoxy resin. Compos B Eng 2020:190.
[43] Yang S, Huo S, Wang J, et al. A highly fire-safe and smoke-suppressive single-component epoxy resin with switchable curing temperature and rapid curing rate. Compos B Eng 2021:207.
[44] Qu Z, Wu K, Jiao E, et al. Surface functionalization of few-layer black phosphorene and its flame retardancy in epoxy resin. Chem Eng J 2020:382.
[45] Chen S, Ai L, Zhang T, et al. Synthesis and application of a triazine derivative containing boron as flame retardant in epoxy resins. Arabi J Chem 2020;13:2982–94.
[46] Maxwell ID, Pethrick RA. LOW-TEMPERATURE rearrangement OF amine cured epoxy-resins. Polym Degrad Stabil 1983;5:275–301.
[47] Cheng J, Wang J, Yang S, et al. Benzimidazolyl-substituted cyclotriphosphazene derivative as latent flame-retardant curing agent for one-component epoxy resin system with excellent comprehensive performance. Compos B Eng 2019:177.
[48] Li Z, Chen M, Li S, et al. Simultaneously improving the thermal, flame-retardant and mechanical properties of epoxy resins modified by a novel multi-element synergistic flame retardant. Macromol Mater Eng 2019:304.
[49] Liu Y, Babu HV, Zhao J, et al. Effect of Cu-doped graphene on the flammability and thermal properties of epoxy composites. Compos B Eng 2016;89:108–16.
[50] Shao Z-B, Zhang M-X, Li Y, et al. A novel multi-functional polymeric curing agent: synthesis, characterization, and its epoxy resin with simultaneous excellent flame retardance and transparency. Chem Eng J 2018;345:471–82.
[51] Baskaran M, Hashim R, Leong JY, et al. Flame retardant properties of oil palm trunk particleboard with addition of epoxy resin as a binder and aluminium hydroxide and magnesium hydroxide as additives. Bull Mater Sci 2019;42.